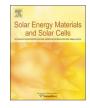


Contents lists available at ScienceDirect

### Solar Energy Materials and Solar Cells

journal homepage: www.elsevier.com/locate/solmat



# Surface fluorination of $\alpha$ -Fe<sub>2</sub>O<sub>3</sub> using selectfluor for enhancement in photoelectrochemical properties



Vikash C. Janu<sup>a,b</sup>, Gaurav Bahuguna<sup>a</sup>, Devika Laishram<sup>a</sup>, Kiran P. Shejale<sup>a</sup>, N. Kumar<sup>b</sup>, Rakesh K. Sharma<sup>a,\*</sup>, Ritu Gupta<sup>a,\*</sup>

<sup>a</sup> Department of Chemistry, Indian Institute of Technology Jodhpur, Jodhpur, Rajasthan , 342037 India
<sup>b</sup> Defence Laboratory (DRDO), Jodhpur, Rajasthan 342011, India

#### ARTICLE INFO

Keywords: Fluorination Hematite Bandgap Photoelectrochemical cell Dendritic DSSC

#### ABSTRACT

Fluorinated α-Fe<sub>2</sub>O<sub>3</sub> nanostructures are synthesized via a facile hydrothermal route using Selectfluor<sup>™</sup> (F-TEDA) as a fluorinating as well as growth directing agent. The addition of incrementally increasing amount of F-TEDA to Fe precursor under hydrothermal conditions resulted in preferential growth of  $\alpha$ -Fe<sub>2</sub>O<sub>3</sub> along (110) orientation with respect to (104) direction by  $\sim$  35%, the former being important for enhanced charge transport. On increasing fluorination, the heirarchical dendritic-type  $\alpha$ -Fe<sub>2</sub>O<sub>3</sub> changes to a snow-flake type structure (F-TEDA-20%) anisotropically growing along the six directions however, at higher F-TEDA concentrations ( $\geq$ 30%), loosely held particulate aggregates are seen to be formed. The X-Ray Photoelectron Spectroscopy (XPS) suggest the maximum fluorinarion of  $\alpha$ -Fe<sub>2</sub>O<sub>3</sub> at 1.21 at% in 30% F-TEDA. Further, optical absorption studies reveal reduction in optical band gap from 2.10 eV in case of pristine to 1.95 eV for fluorinated α-Fe<sub>2</sub>O<sub>3</sub>. A photoanode made by taking 20% fluorinated  $\alpha$ -Fe<sub>2</sub>O<sub>3</sub> in a ratio of 10:90 with respect to TiO<sub>2</sub> (P-25) showed improved performance in dye sensitized solar cells with an increase in efficiency by  $\sim 16\%$  in comparision to that of pristine  $Fe_2O_3$  and  $TiO_2$ . Furthermore, anode consisting of thin films of fluorinated  $\alpha$ - $Fe_2O_3$  on FTO also exhibit enhanced current density on illumination of ~100 W/m<sup>2</sup>. The increase in photoelectrochemical activity seems to be due to the combination of two factors namely preferential growth of  $\alpha$ -Fe<sub>2</sub>O<sub>3</sub> along (110) direction resulting in an improved charge transfer efficiency and reduced recombination losses due to the presence of fluorine.

#### 1. Introduction

Hematite or  $\alpha$ -Fe<sub>2</sub>O<sub>3</sub> is widely used in a variety of applications such as electrode in lithium batteries [1,2], production of magnetic materials [3], visible-light photocatalysis [4–6], water treatment [7], gas sensors [1,8], electromagnetic devices, paints and pigments [9]. High-quality hematite films are mainly fabricated by various techniques such as atmospheric pressure chemical vapor deposition (APCVD), atomic layer deposition, electron-beam, pulse laser deposition, reactive DC magnetron sputtering and metal organic decomposition for use in photoelectrochemical cells [10–13]. Being a highly abundant, low cost and nontoxic material with a low bandgap of 2.1–2.2 eV,  $\alpha$ -Fe<sub>2</sub>O<sub>3</sub> has attracted immense attention in the recent past. However, there are certain drawbacks that limits the use of  $\alpha$ -Fe<sub>2</sub>O<sub>3</sub> in solar application such as low mobility of carriers (< 0.1 cm<sup>2</sup>V<sup>-1</sup>s<sup>-1</sup>) [14] high recombination rates, short diffusion length (2–4 nm) [15], short excited state lifetime (< 10 ps) [16], poor light absorption [17], and improper band position [18] for unassisted water splitting that limit its application in solar applications. There is lot of impetus in improving its properties by structural modification, variation in morphology and by doping [19,20].

Recently, extrinsic fluorine anion doping of semiconducting metal oxides such as SnO<sub>2</sub>, TiO<sub>2</sub>, Co<sub>3</sub>O<sub>4</sub> and Fe<sub>2</sub>O<sub>3</sub> have turned out as an important route for surface passivation of metal oxides that inhibits  $e^{-}/h^+$  recombination and improves charge carriers mobility. Additionally, fluorine doping is expected to achieve tunable optical absorption and modified band position for enhancement in photoelectrochemical activity. Theoretical studies also suggest that the partial replacement of O<sup>2-</sup> by aliovalent anion such as F<sup>-</sup> can effectively reduce the electrical resistivity of Fe<sub>2</sub>O<sub>3</sub> [21]. For example, Tondello et al. synthesized F-doped Co<sub>3</sub>O<sub>4</sub> by plasma enhanced chemical vapor deposition method using fluorinated β-diketonatecobalt derivative as a single fluorine and cobalt precursor and observed a significant improvement in hydrogen production. Similarly, Choi et al. carried out fluorination of TiO<sub>2</sub> using

\* Corresponding authors. E-mail addresses: rks@iitj.ac.in (R.K. Sharma), ritu@iitj.ac.in (R. Gupta).

http://dx.doi.org/10.1016/j.solmat.2017.09.006

Received 28 June 2017; Received in revised form 2 August 2017; Accepted 6 September 2017 0927-0248/ © 2017 Elsevier B.V. All rights reserved.

sodium fluoride for enhanced photo catalytic action [22,23]. The enhancement in catalytic activity is understandable due to increase in Lewis acidity of Fe-centers by substitution of surface oxygen atoms with fluorine. For example, Zhu *et al.* observed rapid photo catalytic degradation of Rhodamine dye using fluorinated  $SnO_2$  [24,25]. Several fluorine-doped metal oxides have been synthesized in order to enhance the electrochemical performance of energy storage devices. Lee et al. synthesized F, N-doped Fe<sub>2</sub>O<sub>3</sub> using ammonium fluoride and urea and used it for supercapacitor application [26].

Among solution-based fluorinating agents, HF and NH<sub>4</sub>F are generally used, however, these act preferentially as growth directing agents with no evidence for fluorination in the growth of metal oxides [27]. Herein, we for the first time, utilized F-TEDA as a fluorinating agent that provides electrophilic fluorine in solution as the reactive species. In this work, we developed a facile yet effective hydrothermal strategy for the in-situ preparation of F-Fe<sub>2</sub>O<sub>3</sub> by modifying the known method for dendritic growth of  $\alpha$ -Fe<sub>2</sub>O<sub>3</sub> [28]. In order to understand the interaction of fluorine with  $\alpha$ -Fe<sub>2</sub>O<sub>3</sub>, we focussed on the interplay between the fluorine content (varying F-TEDA concentration 0–40%) and resulting structural, optical and photoelectrochemical properties together with study on its application in visible light photo-electrochemical and dye sensitized solar cells.

#### 2. Experimental section

#### 2.1. Synthesis of pristine and F-Fe<sub>2</sub>O<sub>3</sub>

Aqueous solution of (15 mM) of  $K_3$ [Fe(CN)<sub>6</sub>] was heated in Teflon hydrothermal vessel (200 mL) at 140 °C for 48 h following the literature method [28]. The precipitate was obtained and washed with de-ionized (DI) water followed by ethanol wash to get rid of the by-products. It was further centrifuged and dried in hot air oven at 70 °C for 4h. *In-situ* fluorination was carried out using Selectfluor<sup>™</sup> (N-Chloromethyl-N'fluorotriethylenediammoniumbis(tetrafluoroborate), F-TEDA, Sigma Aldrich) as the fluorinating agent. F-TEDA was mixed in different weight percent with respect to the principal reactant before the start of reaction.

#### 2.2. Characterization

Bruker D8 Advance diffractometer equipped with Cu-Ka radiation having 1.54 Å wavelength was used for X-ray diffraction (XRD) analysis.  $^{19}\mathrm{F}$  NMR spectra were collected from the reaction mixture before and after reaction (supernatant) in D<sub>2</sub>O using Bruker 500 spectrometer operating at 500 MHz. TEM imaging was performed by transmission electron microscope (FEI Technai G2 T20 ST) equipped with energy-dispersive X-ray spectroscopy (Burker X-100). For imaging,  $\sim$ 10 mg of sample was dispersed in ethanol and drop casted on a copper grid and allowed to dry before imaging. HRTEM images were analyzed using Image J and Gatan digital micrograph software. Field Emission Scanning Electron Microscope (FESEM) imaging was performed using Nova NanoSEM 600 instrument (FEI Co., The Netherlands). Diffuse reflectance spectra were recorded in solid state using UV-vis spectrophotometer (Varian Cary 4000) with polytetrafluoroethylene (PTFE) as the reference material. Surface composition and chemical states were measured with an Omicron nanotechnology (Oxford instruments) X-ray photoelectron spectroscopy (XPS) instrument equipped with monochromatic Al Ka radiation. Specific surface area was analyzed by N2 adsorption-desorption isotherms (Quntachrome autosorb iQ3). Solar Simulator (model number SS50AA, Photoemission Tech) was used to illuminate the devices.

#### 2.3. DSSC fabrication

All solar cells were prepared according to the typical procedure as mentioned in our previous study [29]. Briefly, pristine and  $F-Fe_2O_3$ 

(20%) were mixed with TiO<sub>2</sub> (P25) powders in 5:95, 10:90, 20:80 and 40:60 ratios in the form of a paste and uniformly grinded with ethyl cellulose in  $\alpha$ -terpinol and ethanol (wt% ratio: 2.7:1:3.38). The paste was screen printed on the fluorine doped tin oxide (FTO) substrates and dried at 120 °C for 6 min and repeatedly printed 5 times to increase the laver thickness. The electrodes were sintered at 450 °C for 30 min in the air resulting in film of  $\sim 15 \,\mu m$  thickness with active area of 1 cm<sup>2</sup>. The platinum sol was deposited onto the FTO counter electrode and then calcined at 450 °C for 30 min. The photoanodes were soaked in 0.5 mM N719 dye solution for 18 h. Finally, these were assembled along with Pt counter electrode using a Surlyn spacer (thickness of 25 µm) and Iodolvte Z 50 (Solaronix) as the electrolvte resulting in a sandwich structure as shown in supporting information, Fig. S2a. The fabricated DSSC device was then illuminated under solar simulator 1000 W/m<sup>2</sup> (1 Sun) for J-V and EIS measurements. All the fabricated DSSCs were averaged over three cells.

#### 2.4. Photoelectrochemical measurements

The films of  $\alpha$ -Fe<sub>2</sub>O<sub>3</sub> and F-Fe<sub>2</sub>O<sub>3</sub> were prepared by three layer screen printing on FTO glass for photoelectrochemical measurements. The paste of appropriate viscosity was prepared by mixing 0.05 g of ethyl cellulose, 0.3 mL of  $\alpha$ -terpinol and 0.02 mL glacial acetic acid in a mortar and pestle for 30 min. Upon complete dissolution of ethyl cellulose, 0.1 g of hematite was added and mixed for 10 min. Further, appropriate amount of ethanol was added for viscosity adjustment. The prepared paste was layer by layer coated on FTO glass using 100 mesh screen and squeegee. Every layer was dried before coating successive layer. The prepared films were further annealed at 500 °C for 5 h before using for electrochemical measurements. Electrochemical workstation (CHI6600) was used for I-V measurements and impedance spectroscopy (EIS) analysis in a three-electrode set up using Pt mesh as counter electrode and Ag/AgCl (3 M KCl) as reference electrode. The potential were converted to the reversible hydrogen electrode (RHE) scale using the standard Nernst equation. The graphs were plotted from a frequency range of 1-10<sup>5</sup> Hz. Chronoamperometry experiments were performed at 0.6 V versus Ag/AgCl (1.6 V versus RHE). The measurements were performed under illumination of 100 W/m<sup>2</sup> (one-tenth of 1 Sun) while the light source was switched on and off after every 5 s. The photocurrent value at the end of the chronoamperometry measurement was taken as the steady-state photocurrent and was used to compare different samples.

#### 3. Results and discussion

F-TEDA is a well-known, commercially available, stable fluorinating reagent that acts as a source of *electrophilic fluorine* in organic synthesis [30-32]. In this study, we have employed it for fluorination of an inorganic material, α-Fe<sub>2</sub>O<sub>3</sub> not only due to its high reactivity but also for its ease of handling as compared to the other sources of fluorine such as HF, XeF<sub>2</sub> and F<sub>2</sub> [33,34]. Synthesis is scaled up in different-sized Teflon vessels of 100, 200 and 800 mL capacity as shown in Fig. 1a. The hydrothermal reaction for K<sub>3</sub>[Fe(CN)<sub>6</sub>] was carried out with and without F-TEDA at an optimized reaction condition of ~140 °C for 48 h as detailed in experimental methods. The pH changes in the reaction medium were monitored before and after reaction completion to gain better insight in the process of fluorination (Fig. 1c). The pH of the reaction mixture containing Fe precursor and F-TEDA (10 wt% - 40 wt %) is comparatively lower (pH = 3.4 - 4.0) than Fe precursor in water (pH = 6.2) as the F-TEDA is a salt of strong acid and weak base. However, after the hydrothermal reaction, pH of the supernatant becomes higher due to CN assisted dissociation of water that result in formation of OH<sup>-</sup> ions [35]. For higher concentrations of F-TEDA, the pH of supernatant after the reaction decreases gradually. As seen from Fig. 1c (bottom curve), the overall pH change for the reaction is higher in presence of fluorinating agent (10, 20 and 30 wt% of F-TEDA) as

Download English Version:

## https://daneshyari.com/en/article/6456667

Download Persian Version:

https://daneshyari.com/article/6456667

Daneshyari.com